# Abrasive Wear Modes in Ball-Cratering Test Conducted on $Fe_{73}Si_{15}$ $Ni_{10}Cr_2$ Alloy Deposited Specimen

M.S. Priyan[a], P. Hariharan[a]

[a] College of Engineering, Guindy, Anna University, Chennai-600025, India.

A B S T R A C T

The objective of this study was to develop a theoretical model and associated wear mode map to identify the regimes in which two body abrasion (grooving abrasion) and three body abrasion (rolling abrasion) dominate in the micro-abrasive wear test (also known as the ball cratering wear test). This test is generally considered to be a three body wear test. The wear mechanisms and wear rates were investigated using diamond abrasive over a range of loads (0.05, 0.1 and 0.2 N), and slurry concentrations (0.05, 0.1, and 0.2 volume fraction abrasive). It was found that during abrasion wear, a transition from grooving to rolling wear could be identified for a load with respect to time. The critical condition for the transition between two-body and three-body abrasion was determined from a continuum mechanics model for the penetration of the abrasive particles into the surfaces of the ball and the specimen, coupled with considerations of equilibrium. Two wear modes are usually observed in this type of test: 'rolling abrasion' results when the abrasive particles roll on the surface of the tested specimen, while 'grooving abrasion' is observed when the abrasive particles slide; the type of wear mode has a significant effect on the overall behaviour of a tribological system. Wear rates of metallic samples were determined and the worn surfaces were examined by optical microscopy, SEM and Talysurf profilometry.

## 1. INTRODUCTION

Recently, the micro-scale abrasive wear test has gained large acceptance in universities and research centers, being widely used in studies on abrasive wear of materials, Fig. 1. The micro scale abrasion test (also known as the ball-cratering abrasion wear test), in which the ball is rotated against a specimen in the presence of a slurry of fine abrasive particles, is a useful technique for evaluating the wear resistance of an industrial component [1,2]. There are two main equipment configurations of micro abrasion tests, namely "free-ball" and "fixed-ball". Detailed studies of the influence of test conditions on the wear rates and mechanisms in the test have revealed subtle and initially unexpected effects associated with the influence of ball surface condition on the enhancement of particles [3], and transitions between two body (grooving) and three body (rolling) motion of the particles in the contact. Transitions between

different regimes of particle motion have been mapped and the test conditions which favour either two-or three body abrasions can be defined. Test conditions, suitable for various types of materials can now be recommended [3].
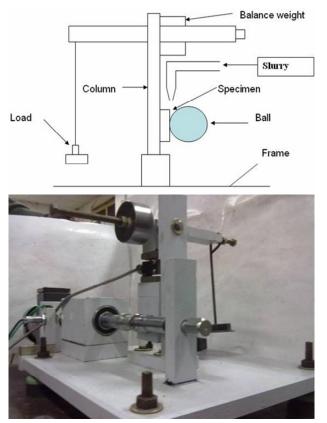


**Fig. 1.** Schematic diagram of micro abrasion tester.

In the micro scale abrasion test, which employs free abrasive particles, two distinct wear modes have been identified [3]. Since wear is a system response and is not a material property, the wear resistance of a material can vary over wide range of different mechanisms are induced by different test conditions [4]. Two abrasive wear modes are usually observed on the surface of the worn crater. The first mode is the rolling abrasion which is the result of the rolling of abrasive particles on the specimen and the second mode is the grooving abrasion which is the result of the abrasive particles sliding on the specimen. The dominant wear modes in the micro-scale abrasion test have been reported to be influenced by applied load, volume fraction of abrasive in the slurry [5]. The type of wear mode has a significant effect on the wear rate of a tribological system [6,7]. In micro scale abrasion wear tests, a rotating ball is forced against the tested specimen, in the presence of abrasive slurry, and the wear behaviour is analysed based

on the dimensions of the crater formed during the test. This test has been applied in the study of the abrasive wear of metallic [10-12] and non-metallic [13-20] materials, depending on the equipment configuration. The ball-cratering micro scale abrasion wear test [21-24] is an example of a test method which produces imposed wear scar geometry. In order to use the ball-cratering method as a standard test to evaluate abrasive wear resistance, it is essential to ensure that either two-body or three-body abrasion occurs in the test; there is some evidence that three-body abrasion leads to more reproducible test results [25].

The dominant process is controlled by the nature of the abrasive particle motion in the contact region between the ball and the specimen. If the particles do not move relative to the ball surface, but act as fixed indenters moving across the specimen, a series of fine parallel grooves is produced on the specimen surface. This leads to so-called grooving wear or two body abrasion. If on the other hand the abrasive particles roll between the two surfaces, indentations with no evident directionality are produced in a process known as rolling abrasion or three body abrasion [26,27].

All the polymers produce relatively low wear rates compared to those obtained with the soft metals. As the hardness of the disc increases, more of the embedded abrasive grains protrude above the surface and the wear rate of the ball then increases, as observed. However, when the disc becomes very hard, tool steel, penetration of the abrasive particles must be very small and they will thus be only weakly attached to the disc surface. These particles can therefore be displaced at the edge of the contact zone, rather than carried into it, and the wear of the carbide ball will be reduced. The existence of a maximum wear rate of the harder material when the softer material reaches a critical hardness is also evident from the results. For polymers, however, the amount of embedded abrasive particles is lesser than the softer metals and appears to vary very little with hardness. As the hardness of polymers decreases, so does the elastic modulus.

In consequence, although particles penetrate the softer polymers more easily, the lower modulus and greater elastic limit of strain tend to displace

the particles again during elastic recovery after the load is removed. The extreme example of this occurs with rubbers where there is little or no retained abrasive at all [28]. The purpose of this work was therefore to formulate a Hertzian contact model for particle motion in the test, and produce an associated wear mode map, plotted using dimensionless parameters, which shows the regimes of dominant wear mode observed in experiments carried out for this project. The wear mode map can then be used to predict the conditions necessary to ensure either two-body or three-body abrasion. In this attempt, a crystalline FeSiNiCr coating was successfully deposited on a gray cast iron substrate by HVOF thermal spraying under controlled conditions, and its wear properties were studied.

In this method, a sphere of radius R is rotated against a specimen in the presence of slurry of fine abrasive particles. The geometry of the wear scar is assumed to reproduce the spherical geometry of the ball, and the wear volume may then be calculated by measurement of either the crater diameter or its depth. For homogeneous bulk materials, the wear volume, V, can be related to the total distance of sliding, S, and the normal load on the contact, N, by a simple model abrasive wear, which is equivalent to the Archard's equation for sliding wear:

$$V = k \, SN \qquad (1)$$

Where k is the 'wear co efficient' with unit's $m^3$ $(Nm)^{-1}$; the abrasive wear resistance is defined as $k^{-1}$ and has units $(Nm) \, m^{-3}$. The usefulness of *k* as a measure of the abrasive wear resistance of the material is thus limited to situations in which the wear volume is directly proportional to both the load and sliding distance. The Wear volume was calculated using the standard technique for measuring the wear scar of spherical geometry [1], i.e. the geometry of the wear scar is assumed to reproduce the spherical geometry of the ball (Fig. 2), and the wear volume (V) may then be calculated by measurement of either the crater diameter (b) or its depth (h):

$$V = \pi b^4/(64R) \quad \text{for } b << R \qquad (2)$$

$$V = \pi h^2 R \qquad \text{for } h << R \qquad (3)$$

A study was therefore carried out in to effect of slurry concentration, abrasive material and applied normal load on the mechanism and rate of wear in the micro scale abrasion wear test.
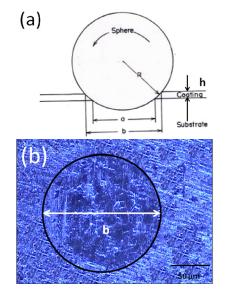


**Fig. 2.** (a) Imposed wear crater depth h (b) diameter b.

## 2. EXPERIMENTAL PROSEDURE

### 2.1 Material and Coating Preparation

Gray cast iron was the desired choice of substrate material, being the most prevalently used material for automotive application which undergoes continuous abrasion and exposure to high temperature in its regular service. The materials and their properties are listed in Table 1.

**Table 1.** Properties of materials used for balls and specimens.

|  | Material | Diameter (mm) | Roughnes, $Ra$ (μm) | Hardness (GPa) | Young's Modulus (GPa) | Poisson's ratio |
|---|---|---|---|---|---|---|
| Ball | EN 31 steel | 25.4 | 0.295 | 9.8 | 198.5 | 0.28 |
|  |  |  |  |  |  |  |
| Specimen | Coated specimen | 24.5 | 0.6 | 6.5 | 220 | 0.18 |

Chemical composition of the selected substrate material is provided in Table 2. Suitable specimens of length 12 mm and diameter 24mm were fabricated from the substrate bar by EDM wire cutting to a nearer size, followed by grinding on both the faces to remove surface irregularities as well as any induced micro-level of heat affected zone that could have resulted from EDM cutting. Surface roughness of the samples was maintained around 6μm by the grinding operation. Raw material for coating, FeNiSiCr alloy powder, was obtained from M/s L&T EWAC powders Ltd., with a pre-mixed composition of Fe-73 %, Si-15 %, Ni-10 % and Cr-2 %. Presence of Ni and Cr alloys improves

wear properties, thermal stability and corrosion properties of coating. The as-atomized powder particles were in the size range from 45 to 55 µm and an appropriate HVOF system was used for spray coating on the substrate. The specimens were thoroughly cleaned with acetone. Spraying parameters to produce a coating layer of about 400µm thickness are presented in Table 2.

**Table 2.** Chemical composition of the substrate and coating.

| Composition (%) | Fe | C | Si | S | Cr | Mn | Ni | P |
|---|---|---|---|---|---|---|---|---|
| Material (Gray cast-iron) | 94.78 | 3.0 | 1.320 | 0.283 | 0.0847 | 0.264 | 0.017 | 0.283 |
| Fe based alloy powder | 73 | - | 15 | - | 02 | - | 10 | - |

## 2.2 Coating Characterization Methods

The HVOF coated samples were polished in a series of coarser to finer grades of silicon carbide emery papers. These samples were further polished with velvet cloth with diamond paste. As a result a micro-polished surface was obtained for further analysis and evaluation. The porosity was identified by PMP3 inverted metallurgical microscope with stereographic imaging and image analyser with Dewinter Material Plus 1.01 software based on ASTM B276. By analysing and averaging various optical micrographs taken at different areas of the coating, as per standard test method, the porosity of the coatings was found to be less than 2 % on the coated surface. The porosity test was followed by wear test. The wear scar morphology study was performed by scanning electron microscope (SEM) equipped with an energy dispersive X-ray analysis (EDX) apparatus.

## 2.3 Wear Test Evaluation

Commercially available micro abrasion tester made by the company Wear and friction Tech (India) Pvt. Ltd. was used for the test in accordance with standard ASTM G 77 (Table 3).

**Table 3.** Micro-abrasion test parameters.

| Substrate | Fe based alloy coated specimen, Surface roughness $R_a$=0.6 µm. |
|---|---|
| Sphere material | High Carbon – High Chromium material conforming to EN 31 Ball diameter-25.4 mm, Surface roughness $R_a$=0.068 µm.Hardness-750 VHN at 100 g load |

| Sliding distance | 150 rev or 11.78 m |
|---|---|
| Load | 0.05, 0.1 and 0.2 N |
| Test Duration | 2, 4, 6 minutes |
| Slurry | Diamond slurry with distilled water, Particle size (<1µm) triangular shape |

The details of the experimental rig as follows. A 25 mm ball is located between two co axial shafts each carried in support bearing. One shaft is driven by a variable speed dc generated motor. The coated samples were pressed against a directly driven steel spherical ball, under a fixed load, rotating at 150 revolutions per minute. The test sample was clamped onto a platform, which is fitted to the pivoted L-shaped arm. This arm was rotated around its pivot until the sample became in contact with the spherical ball. The beam was in balance when the samples were in contact and the load was applied by adding dead weights to a cantilever arm. This configuration has the advantage of accurate control of both normal load and sliding speed. Furthermore the coating was subjected to abrasion with three different loads viz. 0.05, 0.1, and 0.2 N, for duration of 2, 4, and 6 min in each of these loads. Diamond slurry was continuously fed on the interface between the spherical ball and sample throughout the test. Complete test parameters are presented in Table 4.

**Table 4.** HVOF process parameters.

| SI. No | Parameters | Qty |
|---|---|---|
| 1 | Gun type (Super jet Gun) | 1 No |
| 2 | Pressure of Oxygen | 2.5 Kg/cm2 |
| 3 | Pressure of acetylene | 0.6 Kg/cm2 |
| 4 | Torch angle with respect to substrate | 60° |
| 5 | Torch Speed | 12 cm/min |
| 6 | Distance of torch tip from the substrate | 25 mm |

A study was therefore carried out in wear transition to the effects of slurry concentration, abrasive material and applied normal load in the micro abrasion wear test. Abrasive slurry of diamond particles suspended in distilled water was used, at various concentrations between 0.00025 to 0.26 g of abrasive per cubic centimetre of water. The diamond abrasive had a mean particle size of 1µm, as determined by laser granulometry. The slurries were agitated continuously throughout each test to prevent settling of the abrasive particles. The slurries

were fed on to the top of the ball throughout the test at the rate of approximately 0.26 cm$^3$ min$^{-1}$. The worn samples were examined by optical microscopy, scanning electron microscopy and optical profilometry. Moreover, the weight loss was determined by digital sensitive balance, with accuracy 0.0001 g of type XB 220A precisa instrument.

## 3. RESULTS AND DISCUSSION

### 3.1 Wear Mechanism transitions

In an attempt to identify the wear mechanisms taking place in the different conditions, the worn surfaces by SEM were examined. In the case of the diamond slurry, and for deposited coatings, the craters produced by the diamond suspension show deep parallel scratches, with plastically deformed edges, caused by the hard diamond abrasive particles Fig. 3.
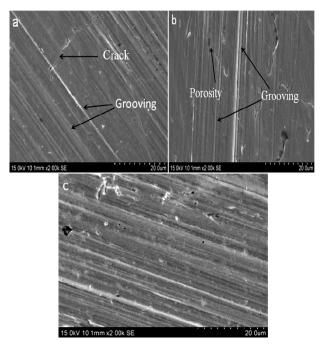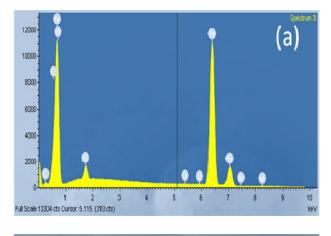


**Fig. 3.** SEM images of the worn surface of a coated specimen produced by micro-scale abrasion at a normal load of (a) 0.05 N (b) 0.1 N (c) 0.2 N with volume fraction 0.05 g cm$^{-3}$ 1μm diamond slurry.
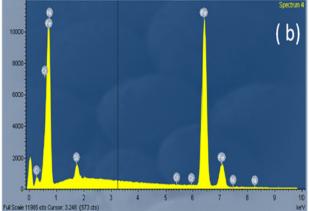
This process occurs when a significant proportion of the slurry particles are embed in the surface of the ball and act as fixed indenters, causing the so-called two body abrasion (or grooving) wear mode. The worn surfaces of Fe based alloy coated specimens from rotating ball as well as unidirectional grooving and rolling

tests were analysed by using scanning electron microscope. The micro cutting action is clearly evident in the coated specimen. Further, in coated specimen, the micro cutting is accompanied by significant micro-ploughing action. The precise cause of this damage is not clearly from the SEM examination.

An optical microscopy analysis of the wear craters obtained in this work indicated that, in all cases, the abrasive wear mode was grooving abrasion: a condition that may be defined as the total projected area of the crater and ($A_g$) as the projected area with grooving abrasion and projected area with rolling abrasion ($A_r$). However, when a more detailed analysis was conducted with the help of a SEM, the occurrence of rolling abrasion was observed along-side the grooving abrasion. A two-body grooving wear mechanism was found to be dominant at high loads and / or low slurry concentrations for all abrasives tested. This process occurs in the micro scale abrasion test when a significant proportion of the particles are embed in the surface of the ball bearing and act as fixed indenters, producing a series of fine parallel grooves in the specimen surface.

Examination of such wear scars by SEM Fig. 3 indicates that the grooves are steep-sided and correspond well in size with the abrasive particles. This suggests that the grooves are formed by the abrasive particles and not by asperities on the surface of the ball. The dominant mechanism at low loads and high slurry concentrations was a three-body process, in which the abrasive particles do not embed, but roll between the two surfaces producing a heavily deformed, multiply indented wear surface with no evident surface directionality.

At intermediate loads and / or slurry concentrations some of the wear scars displayed a mixed character, with two-body grooving in the centre and three-body rolling at the sides. EDX analysis (Fig. 4) indicated that these oxides contained Fe and Si and minor amounts of Cr, in proportions similar to the base alloy composition. The dependence of the wear mechanism on load and abrasive concentration can be explained by an adaptation of an existing model; Williams and Hyncica [24] showed that

an abrasive particle between two surfaces undergoes a transition from grooving to rolling at a critical value of D/h where D is the particle major axis and h is the separation of the surfaces as shown in Fig. 5. In their work, the separation h was determined by hydrodynamic lubrication conditions; in the present case, the surfaces are not supported by a significant hydrodynamic pressure, and so the separation is determined by the load and by the number of particles within the contact.
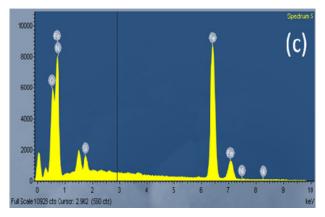


**Fig. 5.** The geometry of a single abrasive particle is described by parameters D and β, after (Williams and Hyncica (24))

### 3.2 Effect of Rolling and Grooving abrasion on the wear mode transition

Figure 6 presents the practical definition of the total projected area ($A_p$), projected area fraction with grooving abrasion ($A_g$) and projected area fraction with rolling abrasion ($A_r$).The optical microscopy image of a wear crater produced during the test applying a load of 0.05 N with a slurry volume concentration of 0.05 gcm$^{-3}$ shows rolling and grooving abrasion (Fig. 6).



**Fig. 6.** Abrasive wear mode: Simultaneous action of rolling abrasion and grooving abrasion.

When the load is increased to 0.1 N for the same slurry volume concentration, the microscopy image shows mixed abrasion (rolling and grooving). The microscopy image shows only grooving abrasion, when the load is further increased to 0.2 N for the same slurry volume concentration. It can be concluded that when a higher load is applied during the micro abrasion test, the diamond particles are not able to roll between the interfacing surfaces of the coated specimen and the ball which results in grooving abrasion. In many abrasive wear mechanisms it



**Fig. 4.** EDS analyses for worn surfaces of Fe based alloy coated specimen subjected to normal loads of (a) 0.05 N, (b) 0.1 N, and (c) 0.2 N at ambient temperature.
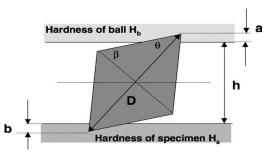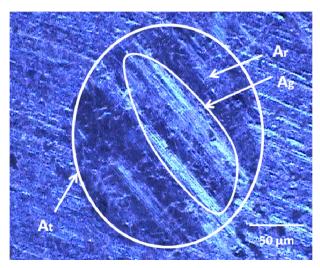
is likely that careful examination of the wear surface would be required in order to determine whether grooving wear or rolling wear in occurring; the classification scheme out-lined above is at a disadvantage with respect to alternatives based on the severity of the wear.

Figure 6 presents the definition of the projected area fraction with grooving abrasion ($A_g$) and the total projected area ($A_p$), respectively. In Fig. 6, areas were defined using the same wear crater, which was generated after a test with the fixed ball equipment, on the $Fe_{73}Si_{15}Ni_{10}Cr_2$ based alloy coated specimen and for a sliding distance of 11.78 m. Using further experimental results for different slurry volume concentrations and for different loads a wear mechanisms map was produced (Fig. 7). The transition between two body grooving and three body rolling was found to occur at an approximately constant ratio of load to volume fraction for the abrasive for load up to 0.2 N.
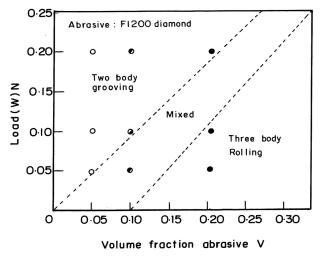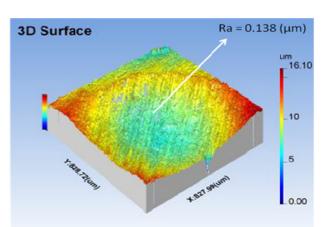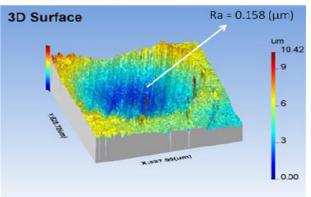


**Fig. 7.** Wear mechanism map for ball crater micro scale abrasion of $Fe_{73}Si_{15}Ni_{10}Cr_2$ alloy coated specimen by sub-micron diamond slurry.

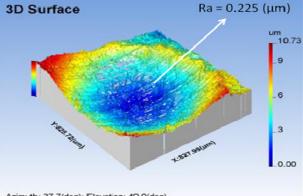### 3.3 Non-contact 3D surface roughness transition analysis

Traditional surface finish analysis consists mainly of studying the surface texture, in terms the surface roughness and waviness, Fig. 8. The main goal of using this analysis procedure was to introduce different types of load surface to represent the original roughness features, thus providing a basic for comparing their performance in contact behaviour. The surface-roughness-3D analysis tests were performed on coated samples. Completely different worn

surfaces were developed in order to establish specific characteristics from which conclusions could be drawn that related the wear process. Another objective was to explain the wear phenomena that were generated in the surface, as indicated in the profile shown in the coating depicted in Fig. 8, the maximum depth of the wear track being 0.108 μm, to measure the mass loss that is determined from the profile.



**Fig. 8.** Wear scar surface finish profile records of coated material (a) Load 0.05 N, $R_a$=0.138 μm, Slurry concentration 0.05 gcm$^{-1}$ (b) Load 0.1 N, $R_a$= 0.158 μm, Slurry concentration 0.1 gcm$^{-1}$ (c) Load 0.2 N, $R_a$= 0.225 μm, Slurry concentration 0.2 gcm$^{-1}$.

It shows the profile traces for coated materials of different initial surface roughness. Only the distance between the predominant peaks rather than the average roughness has a significant effect on the percentage of contact between the metal surface and the coating. As the roughness increases, the distance between predominant peaks increases. Hence, for a given time percentage, the metallic contact for rougher surfaces will be less. This explains the decrease of running-in wear when the roughness ($R_a$) increases from 0.138 μm to 0.225 μm. Figure 8 shows a typical representation of a smooth areal surface texture measurement and also the sampling area refers to the size of the xy plane in which an aerial measurement is performed.

The $R_a$ parameter is the closest relative to the $R_a$ parameter; however, they are fundamentally different and should not be directly compared. Areal, or S-parameters, use areal filters whereas profile, or R-parameters, use profile filters. The $R_a$ parameter is the most common profile parameter for purely historical reasons and the reader should note that $R_q$ is a much more statistically significant parameter than $R_a$. These experiments were carried out using Gaussian filter to test the surface roughness profile from coated surface as per ISO 25178 part 2 [29]. Figure 8 shows a raw measured epitaxial metal surface (a), its short scale SL surface (roughness) (b), middle scale SF surface (waviness) (c) and long scale form surface (form error surface) (d) by using Gaussian filtering with an automatic correct edged process (which has been integrated by some CSI instrument software). Areal surface texture measurement produces a three dimensional representation of a surface. The height data is represented as a height function in a plane, z(x, y).

### 3.4 Wear volumes

A variation of wear volume with slurry concentration was studied for the diamond abrasive and is shown in Fig. 9. It was nonlinear, exhibiting a maximum wear volume at 0.0114 – 0.183 g / cm$^{-3}$ (Volume fraction 0.05 – 0.2) for the loads studied. At low slurry concentrations wear volume was dependent of load, depending predominantly on slurry concentration. The effect of the normal load on the wear volume per unit sliding distance was also studied for both three body rolling and two body grooving

mechanisms, by using the same high (volume fraction = 0.2) and low (volume fraction = 0.05) diamond slurry concentrations to try and ensure that the mechanism stayed the same over the complete range of loads employed.

The wear debris particles were removed from coated specimen at different time due to applied load. Normally the Fe based alloy coated specimen loses minimum debris particles during the test, because of the high hardness and fine dense layered coating deposited. The chart (Fig. 10) shows the average value and standard deviation of weight loss during different duration of time for three loads applied such as 0.05 N, 0.1 N and 0.2 N. The results show that the weight loss was similar for coating applied on substrates of gray cast iron.
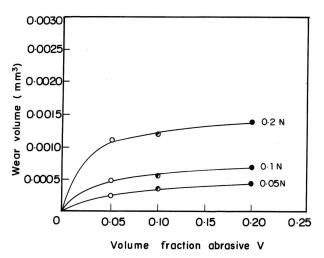


**Fig. 9.** Variation of wear volume after 11.78 m sliding with slurry concentration and applied load in the micro scale abrasion test F1200 sub micron diamond slurry against Fe based coated specimen.
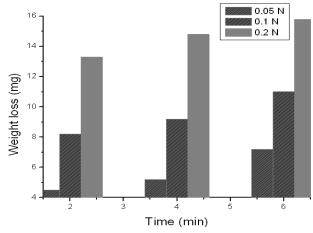


**Fig. 10.** Cumulative weight loss of Fe based alloy coated specimen due to the applied load with respect to time.

## 4. CONCLUSIONS

The results obtained in this work indicated that: In the micro scale abrasion test, both 'two body' grooving and 'three body' rolling mechanisms can be produced in a three body situation, by varying the parameters of normal load, volume fraction of abrasive in the slurry, and abrasive type. The wear mechanism has been mapped for a range of normal loads and volume fraction using diamond abrasive. The grooving mechanism dominated at high loads and low abrasive volume fractions and the rolling mechanism dominated at low loads and high abrasive volume fractions. For the grooving wear mechanism, wear volume is proportional to the normal load, in accordance with the Archard wear equation [1]. Under dry sliding condition, HVOF sprayed FeSiNiCr alloy coating exhibit higher weight loss in this test duration at room temperature. The higher weight loss of as sprayed coating is associated with removal of material by high volume concentration of slurry particles.

## REFERENCES

[1] K.L. Rutherford, I.M. Hutchings: *A micro-abrasive wear test, with particular application to coated systems,* Surface Coating Technology, Vol. 79, N. 1-3, pp. 231-239, 1996.

[2] K.L. Rutherford, I.M. Hutchings: *Theory and application of a micro-scale abrasive wear test,* J. Testing and Evaluation. JTEVA, Vol. 25, No. 2, pp. 250-260, 1997.

[3] R.I. Trezona, D.N. Allsopp, I.M. Hutchings: *Transitions between two body and three-body abrasive wear: influence of test conditions in the micro scale abrasive wear test*, Wear, Vol. 225-229, No. 1, pp. 205-210. 1999

[4] K. Kato, K. Adachi: *Wear mechanisms, in: B. Bhushan (Ed.), Modern Tribology Hand book, CRC press, Boca Raton, FL, 2000*, pp. 273-300.

[5] R.C. Cozza, D.K. Tanaka, R.M. Souza: *Friction co efficient and abrasive wear modes in ball-cratering tests conducted at constant normal force and contact pressure-Preliminary results*, Wear, Vol. 267, No. 1-4, pp. 61-70. 2009.

[6] K. Adachi, I.M. Hutchings: *Wear-mode mapping for the micro-scale abrasion test*, Wear, Vol. 255, No. 1-6, pp. 23-29, 2003.

[7] K. Adachi. I.M. Hutchings: *Sensitivity of wear rates in the micro scale abrasion test to test conditions and material hardness*, Wear, Vol. 258, No.1-4, pp. 318-321 2005.

[8] K. Bose, R.J.K. Wood: *Optimum tests conditions for attaining uniform rolling abrasion in ball cratering tests on hard coatings*, Wear, Vol. 258, No. 1-4, pp. 322-332, 2005.

[9] R.C. Cozza, J.D.B. de Mello. D.K. Tanaka, R.M. Souza: *Relationship between test severity and wear mode transition in micro-abrasive wear tests*, Wear, Vol. 263, No. 1-6, pp. 111-116, 2007.

[10] Y.J. Mergler, H. Huis't Veld: *Micro abrasive wear of semi-crystalline polymers,* Tribology Series, Vol. 41, pp. 165-173, 2003.

[11] R.C. Cozza, R.M. Souza, D.K. Tanaka: *Wear mode transition during the micro-scale abrasion of WC-Co P20 and M2 tool steel,* in: *XVIII International Congress of Mechanical Engineering Proceedings of COBEM Ouro Preto, MG,* (2005), Brazil.

[12] W.M. da Silva, R. Binder, J.D.B. de Mello: *Abrasive wear of steam-treated sintered iron,* Wear, Vol. 258, No. 1-4, pp. 166–177, 2005.

[13] J.C.A. Batista, A. Matthews, C. Godoy: *Micro-abrasive wear of PVD duplex and single-layered coatings,* Surface Coating Technology, Vol. 142-144, pp. 1137–1143, 2001.

[14] J.C.A. Batista, C. Godoy, A. Matthews: *Micro-scale abrasive wear testing of duplex and non-duplex (single-layered) PVD (Ti,Al)N, TiN and Cr-N coatings,* Tribology International, Vol. 35, No. 6, pp. 363–372, 2002.

[15] J.C.A. Batista, M.C. Joseph, C. Godoy, A. Matthews: *Micro-abrasion wear testing of PVD TiN coatings on untreated and plasma nitrided AISI H13 steel*, Wear, Vol. 249, No. 10-11, pp. 971–97, 2002.

[16] A.M. Baptista, J. Ferreira, N. Pinto: *Micro-abrasive wear testing by rotating ball,* in: *Proceedings of the Seventh Portuguese Conference of Tribology*, Porto, Portugal, (in Portuguese), 2000.

[17] J.O. Bello, R.J.K. Wood: *Micro-abrasion of filled and unfilled polyamide 11 coatings*, Wear, Vol. 258, No. 1-4, pp. 294–302, 2005.

[18] T.Z. Kattamis, M. Chen: *Effect of residual stresses on the strengh, adhesion and wear resistance of SiC coatings obtained by plasma-enhanced chemical vapor deposition on low alloy steel*, Surface and Coating Technology, Vol. 70, No. 1, pp. 43–48, 1994.

[19] A. Ramalho: *Micro-scale abrasive wear of coated surfaces-prediction models*, Surface Coating Technology, Vol. 197, No. 2, pp. 358–366, 2005.

[20] E. Robinowicz, L.A. Dunn, P.G. Rusell: *A study of abrasive wear under three body conditions*, Wear, Vol. 4, No. 5, pp. 345-355, 1961.

[21] J. Keller, V. Fridrici, Ph. Kapsa, S. Vidaller, J F. Huard: *Influence of Material Nature and Surface Texturing on Wear of Heavy-Duty Diesel Engine Cylinder Liners*, Tribology Transactions, Vol. 52, No. 1, pp. 121-126, 2009.

[22] J.F. Archard: *"Contact and rubbing of flat surfaces"*, Journal applied Physics, Vol. 24, pp. 981, 1953.

[23] J.A. Williams, A.M. Hyncica: *Abrasive wear in lubricated contacts*, Journal of phys. D. Applied physics, Vol. 25, pp. A81-A90, 1992.

[24] J.A. Williams, A.M. Hyncica: *Mechanisms of abrasive wear in lubricated contacts,* Wear, Vol. 152, No. 1, pp. 57–74, 1992.

[25] J.D. Gates: *Two body and three body abrasion: A critical discussion,* Wear, Vol. 214, No. 1, pp. 139-146, 1998.

[26] D.N. Allsopp, R.I. Trezona, I.M. Hutchings: *The effects of ball surface condition in the micro scale abrasion test,* Tribology letters, Vol. 5, No. 4, pp. 259-264, 1998.

[27] M.H. Staia, C. Enriquez, E.S. Puchi, D.B. Lewis, M. Jeandin: *Application of ball cratering methods to study abrasive wear*, Surface Coating Technology, Vol. 14, No. 1, pp. 49-54, 1998.

[28] J.K. Lancaster: *Abrasive wear of polymers,* Wear, Vol. 14, No. 4, pp. 223-239, 1969.

[29] Richard K. Leach: *Fundamental principles of engineering nanometrology*, Elsevier, USA, 2010.